Digest Journal of Nanomaterials and Biostructures Vol. 11, No. 4, October-December 2016, p. 1035-1044

POROUS COPPER SHEETS DIAGNOSTIC METHODS

C. M. SIMA[a*], V. CIUPINA[abc]
[a]*Department of Solid-State Physics, University of Bucharest, Bucharest-Magurele 077125, Romania*
[b]*Ovidius University of Constanta, Constanta 900527, Romania*
[c]*Academy of Romanian Scientists, Independentei 54, Bucharest, Romania*

Porous copper based materials have excellent conductive and mechanical properties which make them suitable in many applications. In this paper were obtained several porous copper sheets using sintering method in a controlled atmosphere. In order to study copper's final plate porosity, pore size and pore size distribution we used SEM Microscopy, Cone-beam tomography (CBCT), Brunauer – Emmet – Teller (BET) surface analysis and water boiling techniques. Tests results showed 73.4% porosity in a macroscopic structure range between 1.4-5 μm at the surface and 8.56 – 50 μm in cross-section.

(Received July 29, 2016; Accepted October 5, 2016)

Keywords: GDL, PEMFC, Sintering, Porous copper, Porosity, Pore size

1. Introduction

From more than two decades, in all over the world, were implemented different programs to meet the high energy demands due to the demographic increase, especially in the automotive sector where the fossil fuel lack and gas emissions are the capital issues that have to be urgently solved.

Proton exchange fuel cells (PEMFCs) are excellent energy conversion devices, which due to their high efficiencies, zero emissions, fast start-up, high power densities, noiseless, can be a promising alternative for replacing the conventional energy convertors. Outstanding their high manufacturing cost, PEMFCs are still not achievable for the mass production. Developing new materials and novel manufacturing techniques of the gas diffusion media (according to DOE 2016 [1]) can help PEMFCs technology production to meet the efficiency, durability and cost requirements for the mass production terms.

Normally made of carbon (fiber or cloth), the gas diffusion layer (GDL) is making the connection between the channels flow field and catalytic layer.

For this reason, it has many purposes in the fuel cell operating principle: to act like a pathway for the gases that are passing from the flowing plates trough the catalytic layers, to be an excellent current conductor for leading the electrons to the external load, to have good thermal conductivity to guide the accumulated heat through the flow field for being removed from the cell, to evacuate the water that is forming at the cathode side in order to prevent electrode flooding and to be a mechanic support for the electrode-membrane assembly [2, 3].

This carbon-base is by its nature hydrophilic which is damaging the fuel cell because may block the gasses due to the water accumulation at the cathode side.

To avoid this is necessary to cover it with a hydrophobic material, usually PTFE. In this way the GDL will have hydrophilic and hydrophobic pores which will leave access for both, gas and water.

The major problem with this treated GDL is that, at the moment is not known the adequate balance between the hydrophobic and hydrophilic content [2, 3].

*Corresponding author: simacristina21@gmail.com

Porosity, micro and macro pores size distribution and pore diameter are between the most challenging issues of the gas diffusion media (GDM).

Feng-Yuan Zhang et. al. [4] suggested a new type of GDM based on metallic foil. According to their estimation this new technique offers a better control of the porosity and pore size distribution, improving electric and thermal conductivities as well.

In literature have been developed different instruments to diagnose gas diffusion layer`s porosity and pore size ex-situ measurements [5]. Capillary flow porometry, mercury intrusion porosimetry, scanning electron microscopy (SEM), transmission electron microscopy (TEM), synchrotron tomography and BET surface analysis have been proved to be the most efficient diagnostic tools used to investigate these characteristics [2, 5, 6, 7].

A diagnose of a porous copper diffusion media has been investigated in the present paper. The porous structure was obtained by copper sintering technique in Ar-H_2 (95:5) flow gas mixture. Plate's porosity and pores diameter's distribution was characterized using SEM Microscopy, Cone-beam tomography (CBCT) [8], Brunauer – Emmet – Teller (BET) surface analysis [9] and water boiling techniques [10]. A detailed analysis based on the measurement results will be discussed further.

2. Copper sheets manufacturing process

Having excellent thermal an electrical conductivity and good mechanical properties, copper matrixes are widely used in different applications as catalyst supports or heat exchangers. A good way to avoid copper's oxidation and to obtain a porous structure is the sintering technique in a controlled atmosphere, usually hydrogen or a hydrogen mixture [11].

In this experiment, eight copper sheets were fabricated.

The porous copper media was obtained by sintering a mixture of copper fillings (18 g, 23 g respectively) with different amounts of naphthalene (4%, 7%, 9% and 11%) in Ar – H_2 (95:5) gas flow, thermally treated at 900ºC. Particles size was under 450 µ. The copper sheets have a square geometry (using the same steel die presented in article [12]) with 30×30 mm size. The fabrication procedure requires two steps: mixture pressing and thermal treatment.

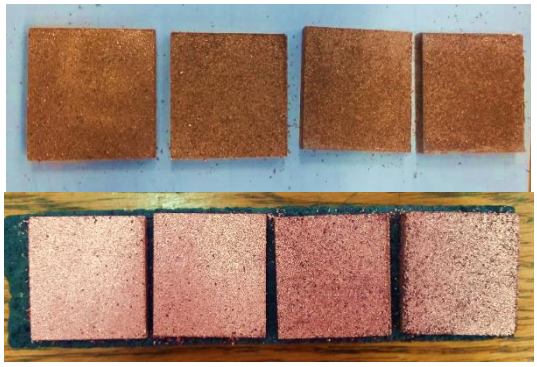

Fig. 1. Copper sheets: pressed (upside) and sintered (downside).

Within the pressure process were made four plates with 18 g of copper mixed with 4%, 7%, 9% and 11%, naphthalene amounts, respectively four plates with 23 grams, all pressed at 15 tonne-force. After pressing the plates were introduced in a tubular furnace [12], in a Ar-H_2 (95:5) gas mixture, with 70 liters/ hour flow rate, in which they were subjected to the following thermal treatment: 350ºC for 5 hours (interval dedicated for the naphthalene removal); 350ºC – 400ºC for 30 minutes and after that we continued to increase temperature with 50ºC at every 20 minutes until we reached 900ºC where we kept it for 30 minutes (Fig. 1.).

3. Results and discussions

As it was mentioned previously in the first section, for the porous sheet characterization we used 4 methods: two for surface investigation (SEM and BET) and two for volume investigation (CBCT and water boiling).

To study the material chemical composition and the naphthalene displacement rate we used EDS and X-ray analysis.

3.1 X-ray and EDS analysis

X-ray investigation was made after and before sintering process of the copper sheets.

As it can be seen in Fig. 2, the registered spectra revealed that after the sintering process the samples have no naphthalene in their structure.

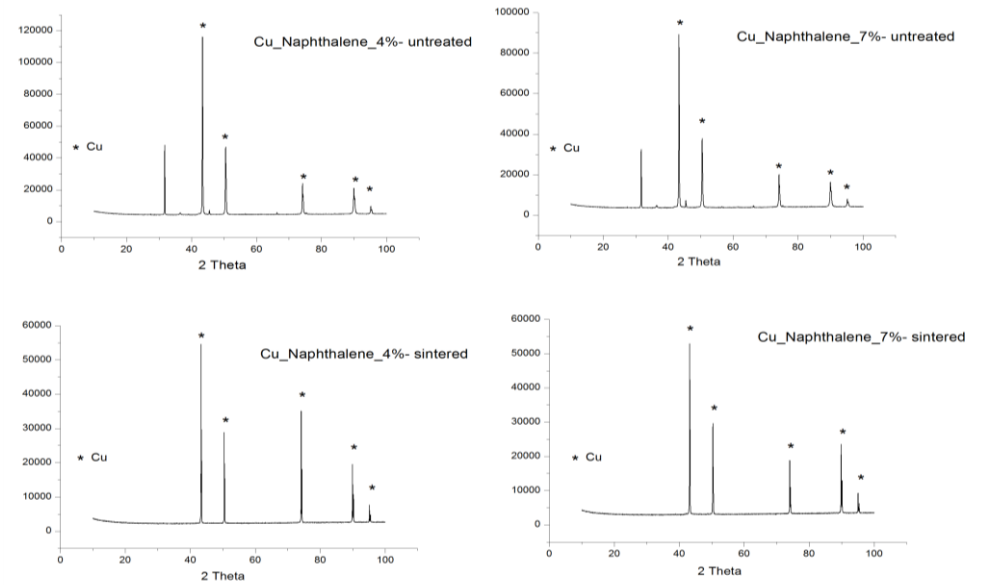

Fig. 2. X-ray diffraction

EDS assay was applied to the samples which contained 7% of naphthalene (Fig. 3).

According to ESD (Fig. 4) test they were identified the following chemical elements: copper amount 96.7%, respectively 91.05%, carbon amount 2.87%, respectively 8.41% and aluminum amount 0.43%, respectively 0.31%.

Aluminum and carbon appearance on the sample surface it is due to the particles diffusion during the sintering process. The aluminum small amounts were deposed as a result of alumina plates diffusion in which the samples were sandwiched to avoid curvature. The identified carbon quantities are showing that during the sintering process one part of the naphthalene amount diffused on the sample surface, without having the possibility to be removed until the end of the process.

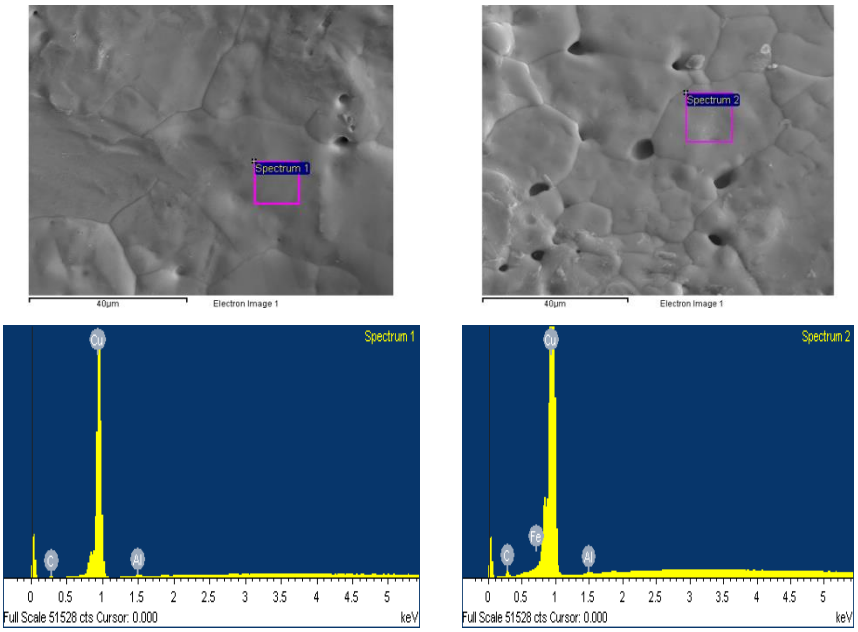

Fig. 3. EDS analysis: Cu 23g (left) and Cu 18 g (right)

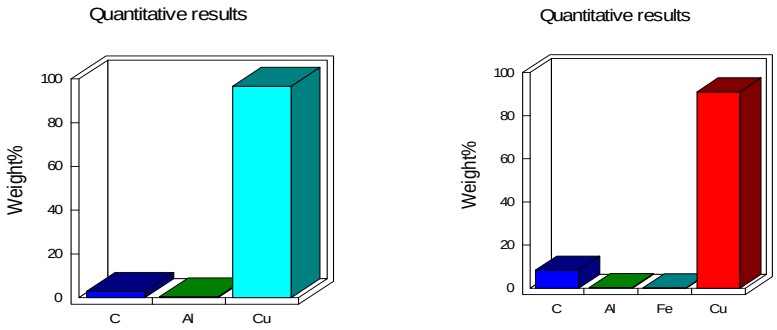

Fig. 4. EDS quantitative analysis of the identified chemical elements: Cu 23g (left) and Cu 18 g (right)

3.2 SEM, CBCT and BET diagnose

Pore size and pore size distribution were investigated by using SEM Microscopy, Cone-Beam Computed Tomography (CBCT) and Brunauer- Emmet-Teller (BET) surface analysis, techniques.

3.2.1 SEM Microscopy investigation

Images that are corresponding with the 7% samples were analyzed using SEM Microscopy.

SEM images were investigated with the help of Image J program. Data acquisition was obtained by using ROI manager of the Image J program.

Data distribution was plotted in Origin Pro 2016 Program.

Fig. 5 and Fig. 6 are representing the subjected areas from the SEM images that were analyzed in the Image J program.

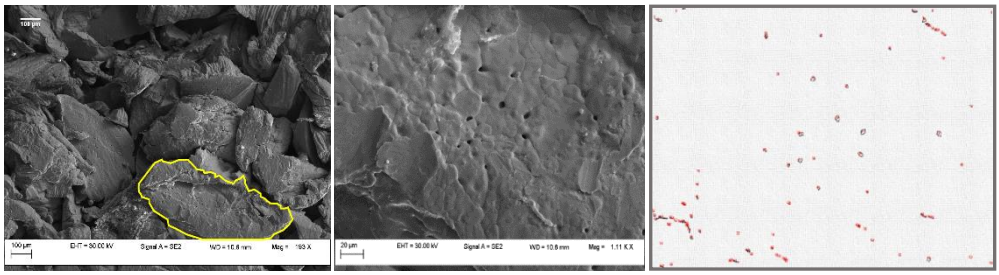

Fig. 5. Analyzed area corresponding to the 7%-18 g sample in Image J program

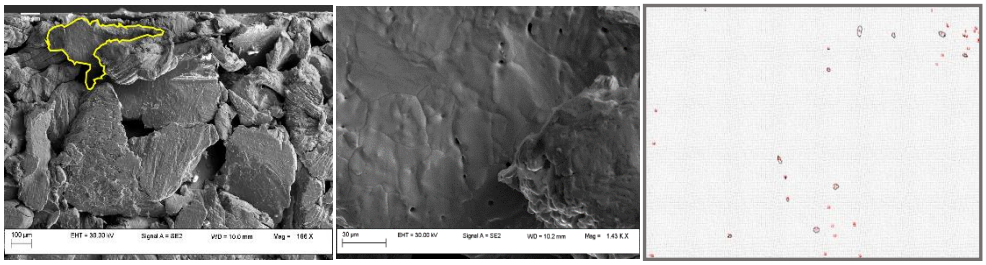

Fig. 6. Analyzed area corresponding to the 7%-23 g sample in Image J program

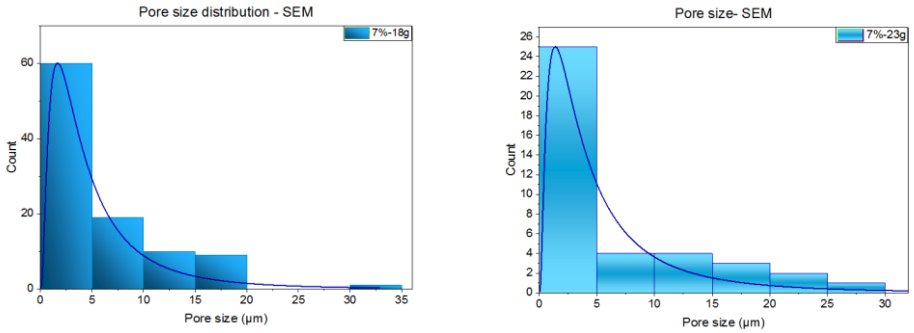

Fig. 7. Pore size distribution upon Image J pore analysis

As it can be seen in Fig. 7, the minimum and maximum registered values of the pore size were between 1.414-35 µm for the 18g sample and 1.4-30 µm for the 23 g sample.

In both cases the most loaded pore size distribution was obtained in the case of pore size values between 1.4-5 µm.

3.2.2 CBCT investigation technique

Within CBCT method 4 samples were analyzed: 4% (18 g, 23 g), 7% (18 g) and 9% (23 g). Before analyzing the samples were sliced from the edge side. Section sizes were between" L ×W×H"- (3-7) × (3-7) × (3-5) mm.

CBCT techniques allows 3D visualization and can determine the cross-sectional pore dimension.

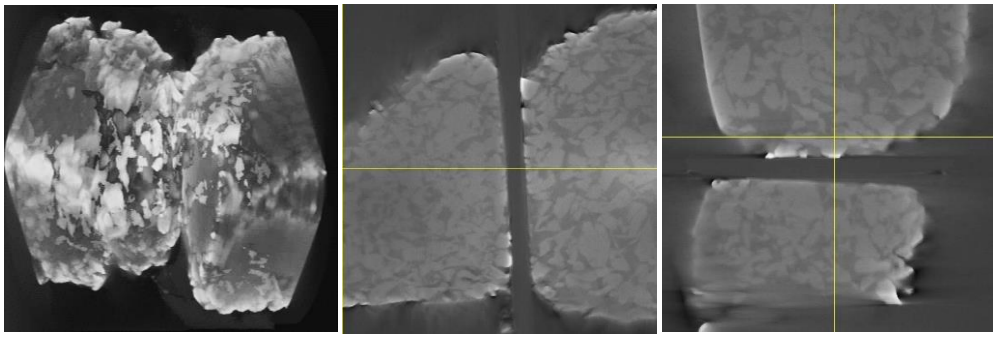

Fig. 8. CBCT images:3D view (left) and orthogonal views(middle-right)

Fig. 9 shows the processing steps that were followed in the Image J program in order to obtain the pore size results.

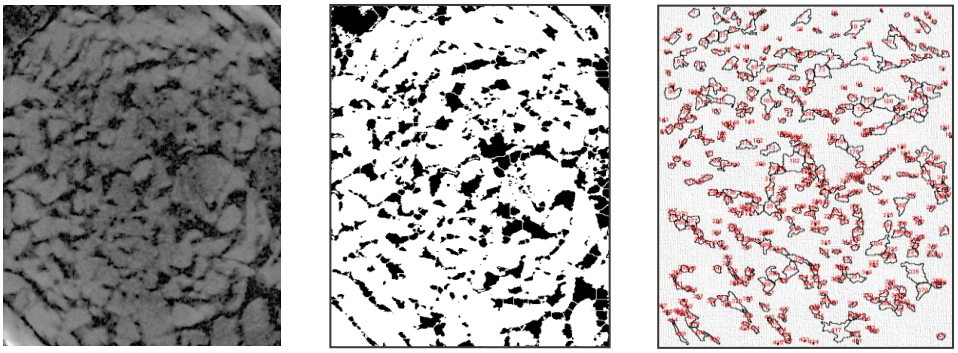

Fig. 9. Processing steps followed for the data acquisition

A threshold adjustment has to be applied to the investigated area before the measuring step. The image scale is in pixels, every pixel having 6.0524284E-3mm. The calculated dimensions (in mm) are plotted in the bottom diagrams (Fig. 10).

According to the diagrams pore sizes are between 8.56-380 μm. The most loaded distribution is around 8.56-50 μm, pores dimensions higher than 200 μm are in a low percentage.

Unlike the pore sizes obtained from the SEM surface analyze, the ones obtained from the cross-section have dimensions higher than 30 μm, reaching the maximum of 320 μm.

Even so, if we compare CBCT results with SEM results we can say that the results (the most loaded distribution) have appropriate distribution intervals.

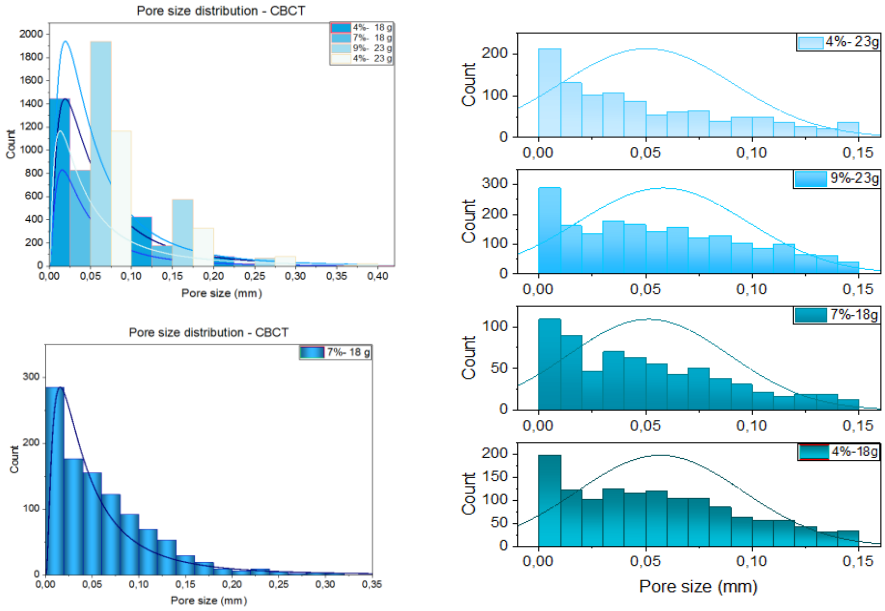

Fig. 10. Pore size distribution diagrams

3.2.3 Brunauer, Emmet, Teller (BET) analyze

In this experiment nitrogen physisorption on the 4% porous solid samples was made in order to determine the BET surface, pore volume and pore size of the copper sheets.

Before starting the experiment, the samples were degassed. The absorption was made at nitrogen boiling temperature (77.383 K), at atmospheric pressure condition and measured with ASAP 2020 instrument from Micrometrics.

The results are registered in the Table 1.

Results have revealed that the sample with 23 g of copper adsorbed a higher quantity of nitrogen comparing with the one with 18 g of copper.

The pores average width (~164 nm) is showing that the porous structure of the 23 g copper sample is predominantly macroporous.

Due to the fact that the 18 g copper sheet did not have a good nitrogen absorption, we could not measure the pore volume and de pore with, revealing that it was a monolayer absorption and the sample has an insignificantly porous area.

Table 1. Summary report of the BET analyzes 4% samples

Sample investigation	***Copper sheet***	
	23 g	***18 g***
Sample initial weight (g)	0.2056	0.279
Sample specific weight (g)	0.1547	0.2778
BET surface area (m^2/g)	0.1871	0.0473
Single point adsorption total pore volume of pores less than 0.0000 nm diameter at p/p° = 1.000510905 (cm^3/g)	0.007681	–
Adsorption average pore width (4V/A by BET) (nm)	164.22519	–

3.3 Copper sheets porosity

In order to determine the samples porosity, we used the oil impregnation method followed by water boiling technique according to the ISO2738/1999 standard.

All copper sheets were measured in this experiment. Room temperature was 23ºC. The samples were dried at 105ºC for 90 minutes, until they reached a constant mass, impregnated in paraffin oil and water boiled for 1 h.

Fig.11 is showing three principal steps followed to achieve the porosity results.

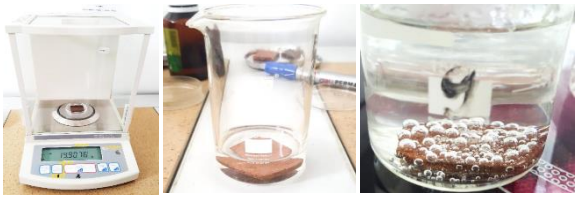

Fig. 11. Porosity experimental determination: dry sample mass (left), sample oil impregnation (middle), sample water boiling (right)

Except of porosity determination, we measure other parameters (sample volume, wet and dry density, water absorption and oil content), according to the formulas that are listed in Table 2.

Table 2. Formulas used for experimental parameters determination

Parameters	***Description***	***Formula***
m_1 (g)	Sample dry mass weighted in air	
m_2 (g)	Impregnated sample weighted in oil	
m_a (g)	Impregnated sample weighted in air	
m_w (g)	Sample mass after boiling weighted in air	
m_3 (g)	Sample mass after boiling weighted in air	
ρ_w (g/cm^3)	Air density	
ρ_{oil} (g/cm^3)	Oil density	
V_s (cm^3)	Volume of the analyzed sample	$V_s = \frac{m_a - m_w}{\rho_w}$
ρ_d (g/cm^3)	Dry density	$\rho_d = \frac{m_1}{V_s} = \frac{m_1 \cdot \rho_w}{m_a - m_w}$
ρ_w (g/cm^3)	Wet density	$\rho_w = \frac{m_2}{V_s} = \frac{m_2 \cdot \rho_w}{m_a - m_w}$
P_{op} (%)	Open pore porosity	$P_{op} = \frac{m_2 - m_1}{\rho_{oil} \cdot V_s} \times 100$
Abs_w (%)	Water absorption	$Abs_w = \frac{m_3 - m_1}{m_1} \times 100$
C_{oil} (%)	Oil content	$C_{oil} = \frac{m_w - m_1}{\rho_{oil} \cdot V_s} \times 100$

The results obtained after applying the formulas above are indexed in Table 3.

Following the data results we can see that samples with low quantity of copper have also a lower open porosity percentage (0.51-24.71%) comparing with the ones with a higher copper

quantity which registered the maximum of 73.4% open porosity. We noticed as well that open porosity percent increased with the oil absorption percentage (> 15%). Densificated samples (4%, 11%-18 g) absorbed small paraffin quantities and achieved low open porosity percentage.
Water absorption range was between 1.66-7.9 %.

Table 3. Diagnostic results of the applied method

Samples	**4% 18 g**	**4% 23 g**	**7% 18 g**	**7% 23 g**	**9% 23 g**	**11% 18 g**	**11% 23 g**
m_1 *(g)*	*15.601*	*19.235*	*12.717*	*22.75*	*19.546*	*17.894*	*23.389*
m_2 *(g)*	*15.736*	*19.776*	*12.945*	*23.438*	*19.945*	*19.015*	*24.55*
m_a *(g)*	*15.791*	*19.889*	*13.085*	*23.539*	*20.11*	*19.095*	*23.74*
m_w *(g)*	*15.757*	*19.797 6*	*12.112*	*22.581*	*19.279*	*18.992*	*23.35*
m_3 *(g)*	*15.86*	*20.236*	*13.225*	*23.763*	*20.165*	*19.308*	*24.926*
ρ_w *(g/cm^3)*	*0.9975*						
ρ_{oil} *(g/cm^3)*	*0.9*						
V_s *(cm^3)*	0.0341	0.092	0.975	0.96	0.833	0.103	0.391
ρ_d *(g/cm^3)*	457.706	209.923	13.037	23.688	23.462	173.294	59.822
ρ_w *(g/cm^3)*	461.667	215.827	13.271	24.404	23.941	184.15	62.791
P_{op} *(%)*	0.511	5.508	24.711	73.417	36.933	12.861	50.436
Abs_w *(%)*	1.66	5.204	3.995	4.453	3.169	7.902	6.571
C_{oil} *(%)*	0.72	6.658	39.884	84.195	52.206	13.779	15.248

Other thing to take into consideration is the fact that similar with BET analyze results, the 4% samples gained the lowest open porosity percentage (0.51% and 5.5%).

4. Conclusions

After the investigation procedures we observed that the sample with 7% -23 g Cu achieved the highest porosity percentage (73.4%) with a pore size average between 1.4-50 µm and pore size distribution range from 1.4-5 µm on the surface according to SEM investigations and 8.56-50 µm upon CBCT analyze. Same sample has a 4.45 % of water absorption, thing which can help in keeping the humidity of the proton exchange membrane.

The high porosity that was achieved together with the excellent thermal and electrical conductivity properties that a sintered copper powder can offer is giving as encouraging reasons to believe that the porous copper sheet can be a good alternative in replacing the carbon-based gas diffusion media, having as well the possibility to make it thinner with low cost production.

Acknowledgements

This work has been funded by the Sectorial Operational Program Human Resources Development 2007-2013 of the Ministry of European Funds through the Financial Agreement POSDRU/159/1.5/S/137750.

References

[1] http://energy.gov/sites/prod/files/2016/06/f32/fcto_myrdd_fuel_cells.pdf (11.06. 2016).
[2] M.Gasik, "Materials For Fuel Cells", CRC Pres, Boca Raton , USA, 130 – 142 (2008).
[3] F. Barbir, "PEM fuel cells: theory and practice", Elsevier, Burlington, 93 – 98 (2005).
[4] Feng-Yuan Zhang, J. Micromech. Microeng. **16**, 23 (2006).
[5] A. Arvay, E. Yli-Rantala, C.-H. Liu, X.-H. Peng, P. Koski, L. Cindrella, P. Kauranen, P.M. Wilde, J. Power Sources, **213**, 313 (2012).
[6] Haijiang Wang, Xiao-Zi Yuan, Hui Li, "PEMFC diagnostic tools", CRCpress, Boca Raton , USA, xviii (2012).
[7] Elina Yli-Rantala, Pauli Koski, Mikko Kotisaari, Sonja Auvinen,Marjaana Karhu, Juha Nikkola, Pertti Kauranen, Arja Puolakka, Pirjo Heikkilä, Advanced Material Solutions for PEM Fuel Cells (Phase 2), Final report, Tampere (2012).
[8] William C. Scarfe, Allan G. Farman, What is Cone-Beam CT and How Does it Work?, Dent Clin N Am, **52**, 707 (2008).
[9] Gobin,Oliver Christian "SBA-16 Materials: Synthesis, Diffusion and Sorption Properties," Laval University, Canada, 2006.
[10] International Standard ISO 2738, "Sintered metal materials, excluding hardmetals – Permeable sintered metal materials - Determination of density, oil content and open porosity" (1999).
[11] Aurelia I. Cuba Ramos, David C. Dunand, Preparation and Characterization of Directionally Freeze-cast Copper Foams, Metals, **2**, 265 (2012).
[12] C. M. Sima, V. Ciupina, G. Prodan, J. Optoelectron. Adv. M. **17**, 602 (2015).